Gadolinium Ions Block Mechanosensitive Channels by Altering the Packing and Lateral Pressure of Anionic Lipids

Yury A. Ermakov,[†] Kishore Kamaraju,[§] Krishnendu Sengupta,[‡] and Sergei Sukharev[§*]
[†]The Frumkin Institute of Physical Chemistry and Electrochemistry, Russian Academy of Sciences, Moscow, Russia; [‡]Indian Association for the Cultivation of Sciences, Kolkata, West Bengal, India; and [§]Department of Biology, University of Maryland, College Park, Maryland

ABSTRACT Effects of polyvalent ions on the lateral packing of phospholipids have been known for decades, but the physiological consequences have not been systematically studied. Gd^{3+} is a relatively nonspecific agent that blocks mechano-gated channels with a variable affinity. In this study, we show that the large mechanosensitive channel MscL of *Escherichia coli* is effectively blocked by Gd^{3+} only when reconstituted with negatively charged phospholipids (e.g., PS). Taking this lead, we studied effects of Gd^{3+} on monolayers and unilamellar vesicles made of natural brain PS, DMPS, and its mixtures with DMPC. In monolayer experiments, we found that μM Gd^{3+} present in the subphase leads to ~8% lateral compaction of brain PS (at 35 mN/m). Gd^{3+} more strongly shrinks and rigidifies DMPS films causing a spontaneous liquid expanded-to-compact transition to the limiting 40 $Å^2$/mol. Pressure-area isotherms of uncharged DMPC were unaffected by Gd^{3+}, and neutralization of DMPS surface by low pH did not produce strong compaction. Upshifts of surface potential isotherms of DMPS monolayers reflected changes in the diffuse double layer due to neutralization of headgroup charges by Gd^{3+}, whereas the increased packing density produced up to a 200 mV change in the interfacial dipole potential. The slopes of surface potential versus reciprocal area predicted that Gd^{3+} induced a modest (~18%) increase in the magnitude of the individual lipid dipoles in DMPS. Isothermal titration calorimetry indicated that binding of Gd^{3+} to DMPS liposomes in the gel state is endothermic, whereas binding to liquid crystalline liposomes produces heat consistent with the isothermal liquid-to-gel phase transition induced by the ion. Both titration curves suggested a K_b of ~10^6 M^{-1}. We conclude that anionic phospholipids serve as high-affinity receptors for Gd^{3+} ions, and the ion-induced compaction generates a lateral pressure increase estimated as tens of mN/m. This pressure can "squeeze" the channel and shift the equilibrium toward the closed state.

INTRODUCTION

Lateral pressure and its transversal distribution in the lipid bilayer attract increasingly more attention as a factor regulating functions of membrane receptors, channels, and transporters (1–3). Although a substantial amount of research is currently focused on the composition of the hydrophobic core of the membrane and resulting pressure profiles (4–7), there has been less attention to modifications in the polar headgroup region that may also exert strong effects on the curvature and resulting pressure distribution.

Mechanosensitive (stretch-activated) channels are the special class of proteins that respond to membrane tension by changing their open probability. Bacterial mechanosensitive channels of MscS and MscL conductance are convenient models, as they permit straightforward reconstitution and respond directly to tension and/or curvature stress in the surrounding lipids bilayer (8–11). The bacterial mechanosensitive channel MscL shows obvious lipid dependence (12), it also activates by asymmetrically incorporated wedge-shaped lysolipids (11). The existing body of data leads to the inference that not only the substances that incorporate into the core of the bilayer and bring extra volume, but also substances that bind externally to the polar region should alter the lateral pressure profile and thus influence the function of integral proteins. Polyvalent ions, and especially triply charged lanthanides (La^{3+}, Gd^{3+}), are known to change packing and phase transition temperatures in lipids, as well as induce phase separation (13,14). Fusogenic, permeabilizing (15–18), and membrane rigidifying (19) effects of lanthanides have been documented as well.

Millet and Pickard (20) and Ding and Pickard (21) were the first to report Gd^{3+} effects on the thigmotropic and gravitropic responses in plants. Soon after, Yang and Sachs (22) reported a blockage of mechanosensitive channels in *Xenopus* oocytes by μM Gd^{3+}, which decreased not only the channel conductance, but also the open probability. The effects were reproduced in cardiomyocytes, astrocytes, and other cells (23,24). One hundred μM Gd^{3+} uncouples osmosensor potential in hypothalamic osmosensory neurons (25). Because Gd^{3+} has the same crystallographic radius as Ca^{2+}, it interferes with multiple Ca-dependent processes (14,26), including membrane fusion (27). Acting in submillimolar concentrations, Gd^{3+} likely exerts its effects by interacting with multiple sites of different affinity, which may not be formed exclusively by proteins but by anionic lipids as well (28).

Submitted April 2, 2009, and accepted for publication November 25, 2009.

*Correspondence: sukharev@umd.edu

Abbreviations used: DMPC, dimirystoyl phosphatidylcholine; DMPS, dimirystoyl phosphatidylserine; EDL, electric double layer; GCS, Gouy-Chapman-Stern approximation; Gd^{3+}, gadolinium; ITC, isothermal titration calorimetry; LE-LC transition, liquid expanded–liquid compact transition; MscL, mechanosensitive channel of large conductance; MscS, mechanosensitive channel of small conductance; PC, phosphatidylcholine; PE, phosphatidylethanolamine; PS, phosphatidylserine.

Editor: Thomas J. McIntosh.

0006-3495/10/03/1018/10 $2.00

doi: 10.1016/j.bpj.2009.11.044

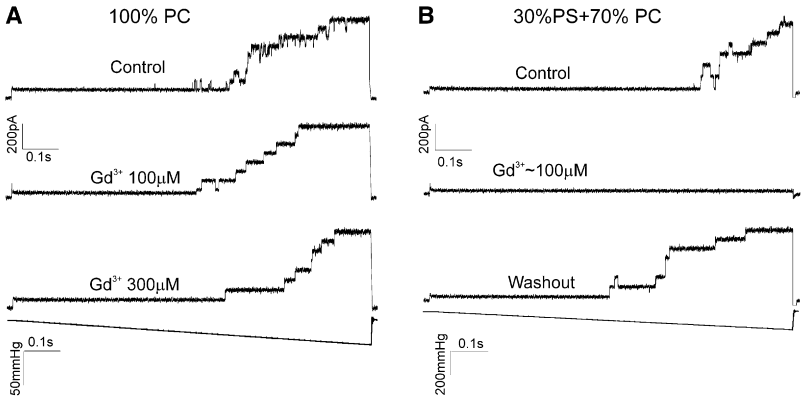

FIGURE 1 Bacterial mechanosensitive channel MscL is blocked by Gd^{3+} when surrounded by negatively charged lipids. (*A*) Current traces of MscL reconstituted with soybean PC recorded at +20 mV (pipette) under a linear pressure ramp (*below*). Perfusion of 0.1 and then 0.3 mM $GdCl_3$ produced a minimal effect on the currents without blocking. (*B*) MscL reconstituted in soybean PC with porcine brain PS (30 mol %) is blocked completely by 0.1 mM Gd^{3+}. The block is reversible as shown by channel reactivation on Gd^{3+} washout.

In bacteria, PS is a metabolic precursor of PE, the major constituent of the cytoplasmic membrane. In mammalian cells, PS represents up to 10% of total phospholipids in the plasma membrane and resides predominantly in the inner leaflet (29). Among other anionic lipids, PS confers a negative net charge to the cytoplasmic face of the membrane necessary for enzyme anchoring and signal transduction (30). Translocation of PS to the outer leaflet, on the other hand, is perceived by the immune system as an alarm signal of injury or death. The lipid was shown to participate in initiation of inflammatory response in the event of necrotic cell death. In other instances, PS triggers silent noninflammatory phagocytosis of cells undergoing apoptosis (31). The exposed PS-rich domains also participate in blood coagulation cascades (32).

The hydrogen-bonding capacity of PE and PS headgroups (33) may explain their predisposition to compact packing in liquid-ordered domains (34). It has been reported that membranes made of synthetic PS are prone to isothermal phase transitions in response to protonation (35), adsorption of Li^+, and especially polyvalent cations (17,36). PS also undergoes phase separation in mixtures with other lipids under similar conditions (37). The specifics of La^{3+} coordination by PS headgroups were studied by Petersheim and Sun (38). Despite many indications that lanthanide ion-PS interactions may be specific and strong, there is insufficient information on binding parameters, the magnitude of electrostatic effects, changes in lipid packing, and mechanical properties of the bilayers.

We have shown previously that planar PS bilayers are highly susceptible to surface modification and restructuring by Gd^{3+}, manifested as a 140 mV increase of the boundary dipole potential. The electrostatic effect was accompanied by a sixfold increase of apparent membrane tension (28,39). In this study, we show that reconstituted mechanosensitive MscL channels can be blocked by Gd^{3+} only when negatively charged lipid (PS) is present in the membrane. The monolayer experiments show a strong compaction of brain PS and especially DMPS monolayers by Gd^{3+}. We investigate effects of Gd^{3+} on the pressure-area (π-A) diagrams and surface (Volta) potentials of DMPS monolayers, relative to neutral monolayer controls. ITC experiments with Gd^{3+} and DMPS liposomes conducted above and below their melting temperature show different thermal effects of ion binding consistent with a phase transition induced by the ion. Based on the analysis of π-A diagrams, we provide estimations of Gd^{3+}-induced changes of lateral pressure in PS domains that explain the blocking of mechanosensitive channels.

MATERIALS AND METHODS

The detailed descriptions of MscL channel reconstitution and recording in the presence of Gd^{3+}, Langmuir monolayer experiments and isothermal titration calorimetry (ITC) are given in the Supporting Material.

RESULTS AND DISCUSSION

MscL is blocked by Gd^{3+} only in the presence of negatively charged lipids

Fig. 1 *A* depicts traces of mechano-activated MscL currents recorded in practically neutral PC liposomes in a control buffer and after addition of submillimolar Gd^{3+}. The three sequential traces are recorded with the same 1-s linear ramp of stimulating pressure, 5 min after Gd^{3+} perfusion to allow for proper mixing and binding. Apart from removing short flickering events seen in the control trace, Gd^{3+} produces no inhibitory effect on channel activity. A set of similar traces obtained in PC/PS liposomes (Fig. 1 *B*) indicates a complete blockage by 100 μM Gd^{3+} and a clear reactivation on washout. The blocking effect was reproducibly observed already at 30 μM. Note that in this experiment we used soybean PC and porcine PS, because with the acyl chain composition found in native mixtures liposomes form more easily and patches are stable. Previous reconstitution experiments carried out with imaging of patches indicated that MscL activates in soybean lipids at tensions between 10 and 12 mN/m calculated from the pressure gradients (~50 mm Hg) and curvature radii (~5 μm) of spherical patches adhered to the glass pipette (9). The reproducibility of responses to 1-s pressure ramps in each of the trials (Fig. 1) shows that the patch does not change its position

in the pipette, as was observed previously under sustained stimuli (9).

The presence of negative charges at the membrane surface could potentially attract more Gd^{3+} to the double layer, increasing its local concentration near the membrane; thus, the protein would effectively see more Gd^{3+} in the latter case. However, the contribution of 0.1 mM Gd^{3+} to ionic strength at the background of 200 mM KCl and 40 mM Mg^{2+} is rather small. Although participating modestly in surface charge screening, Gd^{3+} can neutralize surface by direct adsorption to phosphatidylserine, which may affect mechanical properties of the lipid bilayer and prevent channel opening. The lipid-binding hypothesis is more consistent with our previous observations in planar bilayers (28) and it motivated the following monolayer and ITC experiments.

Mechanical and electrostatic properties of phosphatidylserine monolayers in the presence of Gd^{3+}

It has been reported previously that ion binding and neutralization of charges at the lipid-electrolyte interface can be accompanied by changes in lipid packing and even isothermal phase transitions (36,40–42) We first chose the same porcine brain PS, a partially unsaturated mixture composed primarily of C18:0 (42%) and C18:1 (34%) fatty acids (http://www.avantilipids.com). Fig. 2 depicts a series of pressure-area (π-A) isotherms obtained with the background electrolyte, with 0.1 mM Ca^{2+} and with three different concentrations of Gd^{3+} in the subphase. The control curve shows a ''shoulder'' suggesting that some components in the mixture, possibly saturated, may undergo an LE-LC phase transition with compression. This shoulder is enhanced in the presence of polyvalent ions. Ca^{2+} noticeably changes the position of the isotherm at low π, but near the monolayer-bilayer equivalence pressure of 30–35 mN/m (43), the isotherm converges with the control one. Gd^{3+} at 1 μM noticeably shifts the entire curve to the left. Increasing its concentration to 10 and 100 μM further shifts the isotherm leading to an 11% decrease of molecular area at 35 mN/m. The area compressibility modulus (C_s^{-1}) (44) at these pressures changes from 92 in control to 132 mN/m in the presence of 10 μM Gd^{3+}. The effects of 10 and 100 μM Gd^{3+}on isotherm positions are similar signifying binding saturation, whereas the position of the 1 μM Gd^{3+} isotherm roughly corresponds to half-saturation. During the measurement at the highest concentration of Gd^{3+} we reversed the motion of the barrier before the point of collapse. The forward and backward isotherms coincide showing a hysteresis only at low π (no shoulder in the reverse direction). This illustrates that compaction of the natural PS mixture in the presence of Gd^{3+} is generally reversible. The polyvalent ions markedly decreased the area under the π-A isotherms representing the reversible work of two-dimensional lipid compression. The integrals taken between 58 and 125 A^2/lipid indicate that 100 μM Ca^{2+} and 10 μM Gd^{3+} produce mechanochemical effects of 0.76 and 2.2 kJ/mol of lipid, respectively, aiding compaction.

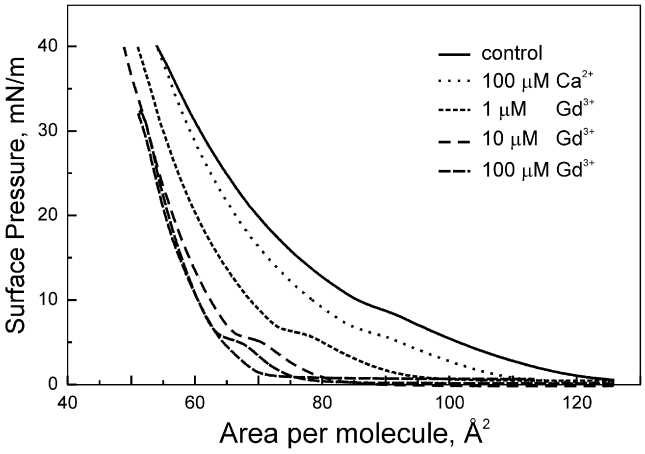

FIGURE 2 Pressure-area isotherms for porcine brain PS monolayers in control (*black*) and in the presence of Ca^{2+} and Gd^{3+} ions. The isotherm for 100 μM Gd^{3+} was measured in both directions and shows reversibility with the exception of small shoulder observed with compression. At the monolayer-bilayer equivalence pressure of 35 mN/m the molecular areas are 57.3, 56.5, 53.0, and 50.6 Å^2, the areas under the curves (integrated between 58 and 125 Å^2/lipid) are 702, 547, 290, and 157 Å^2 × mN/m, and the area compressibility (C_s^{-1}) at 35 mN/m are 91.8, 112.2, 132.4, and 131.5 mN/m for control, 100 μM Ca^{2+}, 1 μM Gd^{3+}, and 10 μM Gd^{3+}, respectively. All isotherms are taken at a barrier speed of 25 cm^2/min on a 600 cm^2 trough.

We then studied DMPS, with a well-characterized phase behavior near ambient temperatures (45). In monolayers, DMPS exhibits a clear LE-LC phase transition on lateral compression (42). The system permitted us to measure pressure-area diagrams at different concentrations of adsorbing ions in the subphase while monitoring the state of headgroup ionization (EDL) and dipole potentials.

Several ''benchmark'' measurements presented in the supplement provided us the scale of effects caused by simple neutralization of DMPS charges with acid, by interacting with a 1:1 monovalent electrolyte or by mixing with neutral DMPC. Fig. S1 *A* depicts a series of pressure-area (π-A) isotherms obtained at different pH values. At neutral and basic pH (7–9), the compression isotherms coincide and show an LE-LC transition at around 25 mN/m signifying high electrostatic repulsion and a maximally charged state of the molecules in the film. A decrease of pH delays the pressure onset on compression and decreases the phase transition pressure to ~7 mN/m. The surface potential curves (Fig. S1 *B*) shift up with progressive neutralization. At pH 2 the surface charge of PS should be close to zero (46,47), and the total surface potential should be represented only by the dipole component, which increases as the lipid packing becomes tighter.

The second benchmark experiment (Fig. S2) illustrates the effect of charge density variation achieved through different PS/PC content in the lipid mixture. The compression

isotherm for pure DMPC shows no LE-LC phase transition (48), which is present in pure DMPS. The mixtures display intermediate behavior. Before the onset of phase transition, the compression isotherms for DMPC and DMPS essentially coincide, indicating that the headgroup specificity starts playing its role in packing at the molecular areas <0.6 nm^2. Higher compressibility of DMPS is apparently conferred by its smaller headgroup capable of hydrogen bonding (35,49). The slopes of surface potential curves also change with the onset of the phase transition, which is pronounced only at high DMPS/DMPC ratios. In our previous study (28) the dipole potential at the surface of the planar lipid membrane became sensitive to the presence of polyvalent ions also when the fraction of charged PS was >50%.

In the third benchmark experiment, we varied the concentration of KCl in the subphase to see the effects of the surface charge screening (Fig. S3), expecting a reduced repulsion with increased ionic strength. At pH 6, we observed that in fact the lowest concentrations of electrolyte (10^{-3} M) produced more easily compressible films with lower transition pressures, whereas higher KCl concentrations produced control-like curves. The positions of surface potential curves (Fig. S3 *B*) indicated 50 mV upward shifts per tenfold increase of salt concentration. This suggests that KCl behaves almost like an indifferent electrolyte. We explain the increased ''stiffness'' of monolayers at higher KCl concentrations as a result of competition between K^+ and H^+ binding to PS considered previously (28,50). Increasing K^+ concentration likely liberates protons from the surface and increases the charge density, which in turn makes the film stiffer. At pH 9–10, when PS headgroups are completely ionized, compression isotherms do not change their shape with ionic strength (not shown).

The benchmark experiments show that neutralization of the surface charges indeed makes the monolayer softer and more prone to isothermal phase transition to the liquid compact state. At 35 mN/m, neutralization of DMPS by acid (Fig. S1) shrinks the area per headgroup by ~10% compared to a fully charged monolayer (0.43 nm^2 at pH >7 vs. 0.39 nm^2 at pH <4). In all experiments, compression of the DMPS film was fully reversible at every pressure or area, i.e., the monolayer was able to expand back.

Introduction of Gd^{3+} in the subphase produced more dramatic effects on mechanical properties of DMPS monolayers than could be caused by simple neutralization of its charges. Fig. 3 depicts π-A and V-A diagrams for a control DMPS monolayer and monolayers in the presence of various (1–100 μM) concentrations of Gd^{3+}. For comparison, experiments on zwitterionic DMPC in the presence of Gd^{3+} are presented on the same graphs. In all experiments, Gd^{3+} made DMPS monolayers extremely rigid, as was concluded from two qualitative observations: the movement of the compressing barrier caused a simultaneous movement of the Wilhelmy plate, and no relaxation of the Wilhelmy plate position was observed on turning it about the connecting wire until

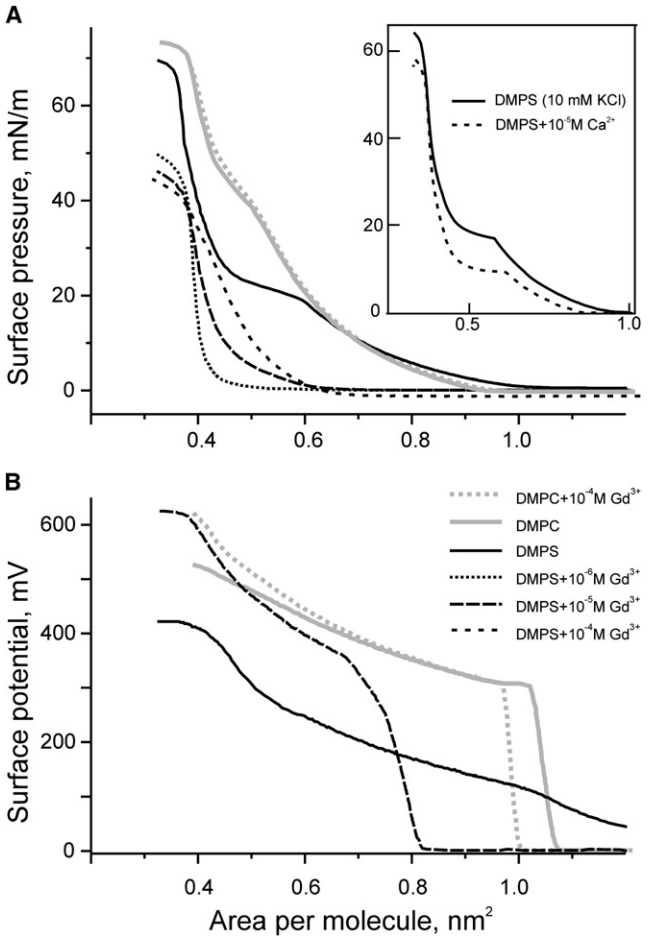

FIGURE 3 Effects of Gd^{3+} on the compressibility (*A*) and surface potential (*B*) of monolayers made of DMPS and DMPC. In *B*, surface potential traces are shown only for control and 10^{-5} M Gd^{3+}, the latter essentially coincided with curves for 10^{-6} and 10^{-4} Gd^{3+}. In all measurements the subphase electrolyte contained 10 mM KCl, 1 mM 2-(*N*-morpholino)ethanesulfonic acid buffer, pH 7.0. Coding of the traces is given in *B*. The inset in *A* represents the effect of 10 μM Ca^{2+} on the DMPS monolayer in the same background electrolyte.

the monolayer was expanded back above the area corresponding to zero surface pressure. The rigidified monolayers thus appeared not liquid any more, but rather solid, as they obviously acquired a nonzero shear modulus. At 1 μM Gd^{3+} in the subphase, the π-A diagram shifts to the left, attaining the minimum possible area per molecule of 0.4 nm^2 at lateral pressures as low as 10 mN/m. Comparing with the control curve, one may see a 44% and 6% compaction at 10 and 35 mN/m, respectively. The pressure in that region of the π-A diagram dropped practically to zero. The area compressibility modulus (C_s^{-1}) determined from the slope of isotherms near 35 mN/m increases from ~150 in control to ~400 mN/m in the presence of 1 μM Gd^{3+}. No strong rigidification of monolayers was observed with 10 μM Ca^{2+} (Fig. 3, *inset*), whose presence exerted an effect similar to partial neutralization at pH 4 (Fig. S1). Compared to that, the effect of Gd^{3+} was considerably stronger. In the presence

of 10^{-5} Gd^{3+}, monolayers of dimirystoyl phosphatidylglycerol exhibited a compaction similar to that of DMPS (data not shown).

The highest degree of compaction achieved with 1 μM Gd^{3+} but not with higher concentrations (10 and 100 μM) seemed unexpected. Our observations suggested that lower apparent compressibility of the monolayer at higher Gd^{3+} can be explained by collisions between rigid domains or clusters at the surface. Acting as a cross-linking agent Gd^{3+} apparently causes clustering of lipids. At Gd^{3+}concentrations >1 μM, exchange of lipids between clusters may be slower than the timescale of compression experiments, and thus domains may collide like ice-floes, unable to compact completely. At [Gd^{3+}] <1 μM, on the other hand, we faced the problem of kinetic limitations, apparently due to slow diffusion of the cation to the surface. On fast compression of a DMPS monolayer to 0.5 nm^2/molecule in the presence of 0.3 μM $GdCl_3$, the pressure reached its peak and then relaxed to a lower level in the course of 2–3 min, thus complicating the measurements.

On adding Gd^{3+}, surface potentials of DMPS monolayers positively shift by ~150 mV relative to the respective potential in the Gd^{3+}-free background electrolyte (Fig. 3 *B*). This vertical shift of the entire isotherm is consistent with the mostly neutralized surface charges, and it is comparable to previous electrophoretic measurements of EDL reduction with Gd^{3+} (114 mV for bovine PS liposomes (28)). On the other hand, compression of the film causes the surface potential to increase monotonously with a slope much higher than predicted for the EDL based on the increasing charge density. Because 10^{-5} M Gd^{3+} is near the zero-charge point for PS (28), the charge density should not change visibly with compaction. The strong rise of surface potential with monolayer compression depicted in Fig. 3 *B* was ascribed to the increased density of individual dipoles at the surface (51). This explanation would be straightforward when ion adsorption does not change dipole moments of lipids. As will be shown below, the dipoles of individual PS molecules are affected by Gd^{3+} only modestly.

From Fig. 3 it becomes obvious that charge neutralization and compaction can evoke a large change of total boundary potential at the membrane interface involving both the diffuse and dipole components. Let us consider a pure PS bilayer where molecules occupy ~0.6 nm^2. Based on the slope of V-A isotherms (Fig. 3 *B*), a Gd^{3+}-induced change of area per headgroup from 0.6 to 0.4 nm^2 should increase the dipole component by ~200 mV. When summed up with an ~150 mV change in the EDL component due to neutralization, the entire change can easily exceed 300 mV. This explains perfectly the changes observed previously (250–320 mV) in the total boundary potential measured in planar lipid bilayers with the inner field compensation technique in the presence of Gd^{3+}, whereas the changes of the diffuse EDL component measured electrophoretically under similar ionic conditions were considerably smaller (100–120 mV) (28).

Analysis of dipole moments from the area dependency of Volta potential

The above surface potential measurements indicated that the compression of the monolayer from 0.7 to 0.5 nm^2/mol in the absence or in the presence of Gd^{3+} induces a change of the surface potential by ~120 mV. The denser packing of surface dipoles in both instances well accounts for the boundary potential changes, in accordance with the Helmholz equation. As described by Brockman (52), surface potentials for monolayers in the expanded state generally obey equation

$$V = V_o + 12\pi\mu_\perp A^{-1},$$

where V_o (mV) is the area-independent contribution, $\mu_\perp$ (mD) is the dipole moment of a molecule and A (A^2) is the occupied area per molecule. The slopes of V-A^{-1} isotherms show that DMPS and DMPC in the expanded state are characterized by similar dipole moments ($\mu_\perp = 0.55$ and 0.57 D, respectively). For both lipid species, $\mu_\perp$ increased by ~18% in the presence of 10^{-5} M Gd^{3+} (Fig. 4). The surface charge of DMPC at this concentration of Gd^{3+} remains close to zero (28), and we should not expect any variation of charge density. Keeping in mind that the large dipole moments of the headgroup are typically oriented parallel to the membrane plane (53), we conclude that Gd^{3+} binding may lead to only a small reorientation of the headgroups. Part of the dipole moment change can also be ascribed to reorientation of the glycerol backbone, aliphatic tails, as well as solvation water (54,55). It is surprising that the individual dipole moment of DMPS, which is a strong ion binder, is the same as for DMPC, a notably weak binder of Gd^{3+}. However, this conclusion was based on the linear region only (Fig. 4). Apart from that region, the dipole

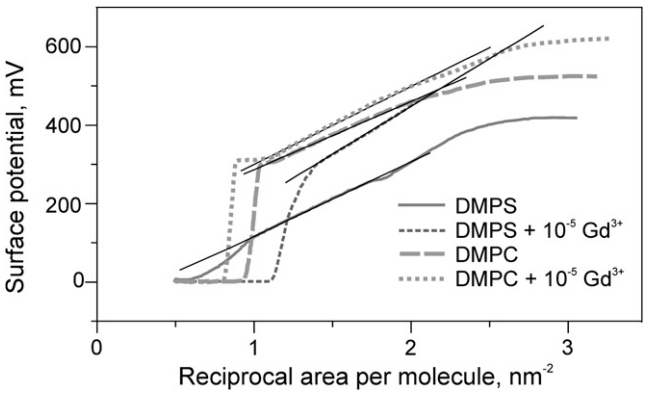

FIGURE 4 Variation of the surface potential with the density of molecules in the DMPS and DMPC monolayers as measured in pure buffers or in the presence of 10^{-5} M Gd^{3+}. Linear stretches of the curves reflect gradual density increase of particles characterized by a constant dipole moment in accordance with equation $V = V_o + 12\pi\,\mu_\perp A^{-1}$. Fitting of these slopes yielded $\mu_\perp$ values for DMPC, 0.46 D; DMPC + Gd^{3+}, 0.53 D; DMPS, 0.55 D, and DMPS + Gd^{3+}, 0.65 D.

potential changes in a nonlinear fashion that may reflect stronger dipole reorientation.

Isothermal titration calorimetry experiments

Unilamellar DMPS liposomes extruded in 10 mM KCl background electrolyte were equilibrated in the calorimeter cell at either 25°C or 45°C. Fig. 5 shows the thermograms and the graphs of integrated heat responses obtained at each temperature. The two series illustrate that the enthalpy of the reaction has different signs and vastly different amplitudes. Interaction of Gd^{3+} with gel-like ''cold'' DMPS is accompanied with moderate heat consumption ($\Delta H > 0$), suggesting that the binding under such conditions is entropically driven. Fitting showed that ΔS is positive suggesting that Gd^{3+} binding in this case is likely accompanied by a liberation of water, solvating the charged headgroups and ions themselves, as well as by liberation of competing K^+ ions. In contrast, Gd^{3+} binding to ''liquid'' DMPS liposomes releases large heat initially, but then after a gradual saturation of the surface, the reaction changes to slightly endothermic before the thermal effect vanishes (Fig. 5 *B*, *open circles*). This character resembles the effect of the myelin basic protein binding to PS liposomes reported previously (56). The initial exothermic phase shows the heat effect that is considerably larger than typical values observed for high-affinity ion binding to macromolecules (57) and is accompanied by a large entropy decrease ($\Delta S = -580$ cal/molK). Assuming that one Gd^{3+} binds to three PS moieties, the overall heat of ~20–25 kcal/mol of injectant gives ~6.7–8.3 kcal/mol of lipid, which corresponds well to the 7.5 kcal/mol enthalpy of gel-to-liquid phase transition for DMPS (45). This immediately suggests that addition of Gd^{3+} into DMPS suspension causes a massive lyotropic phase transition. Based on the previous data obtained with other ions (58), the Gd^{3+}-induced shift in transition temperature likely exceeds 100° and may not be measurable with conventional low-pressure DSC equipment. The ITC curves show that the released heat starts declining at the absolute Gd^{3+} concentration in the chamber ~0.04 mM and vanishes at 0.06 mM. The previous electrophoresis experiments on PS liposomes and intramembrane field compensation measurements in planar bilayers (28) indicated that 0.05 mM Gd^{3+} corresponds to the zero-charge point, after which the binding is impeded due to a surface charge reversal to positive. The correspondence between the saturating concentrations of Gd^{3+} revealed by ITC and the previous electrophoretic titration (28) indicates that the assumption of 1:3 stoichiometry satisfying surface electroneutrality is reasonable. This additionally supports the conclusion that the magnitude of the thermal effect when counted per mole of lipid is very close to that of phase transition for DMPS.

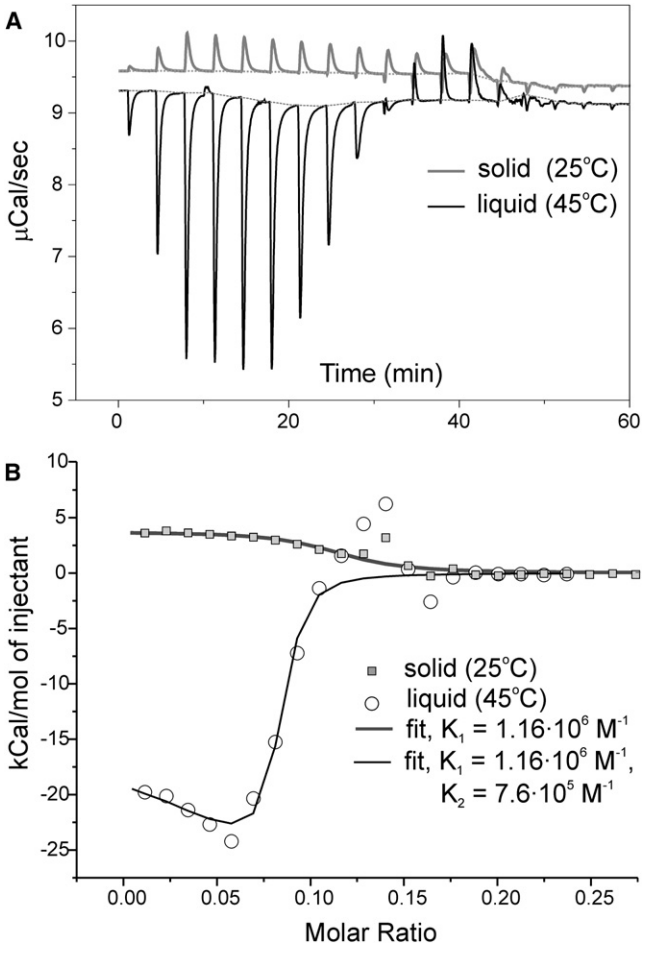

FIGURE 5 Isothermal titration of extruded DMPS liposomes with Gd^{3+}. Two aliquots of the same suspension were equilibrated below T_m (25°C, gel state), and above T_m (45°C, liquid state). In both cases the syringe was loaded with 1 mM $GdCl_3$ and the responses were measured with 5 μL injections (except first two, which were 2 and 3 μL). (*A*) Original thermograms of (*upper trace*) gel and (*lower trace*) liquid liposomes. Note that Gd^{3+} binding to solid DMPS is an exothermic reaction, whereas binding to liquid membranes causes massive heat release (~7 times heat consumption in the former case). However, at the end the heat effect changes its sign to positive. Saturation in both cases occurs at ~60 μM Gd^{3+} in the chamber. (*B*) Integrated heat responses fitted with a single-site model (gel), and a two-site model (liquid).

Fitting of the cold isotherm with a single binding site model produced $K_b = 1.16 \times 10^6$ M^{-1}. Then, having this value fixed for one binding site, a two-site model was applied to the ''melted'' liposomes, which revealed the second type of binding sites with a slightly lower K_b (~7.6×10^5 M^{-1}). This would be consistent with the idea that if ion binding compacts the lipids around the binding sites, initially binding may occur with a lower affinity. Then, when the optimal distance between the headgroups is achieved, the affinity increases. The lipid compacting reaction, which created the high-affinity sites, may involve a certain degree of cooperativity (i.e., very low concentrations of Gd^{3+} may not be able to induce phase transition) because the formation of high-affinity binding sites may depend on the state of neighboring lipids. The fitting procedure also suggested that the number of available binding sites is about an order of magnitude less than lipid molecules present in the cell. The reasons

include: i), at least three PS headgroups constitute a binding site; ii), the molecules forming the inner leaflet of liposomes may not be accessible; and iii), there might be a fraction of binding sites occupied by other cations.

Estimation of lipid lateral pressure acting on the protein inclusion

We showed previously that the opening transition of MscL is associated with a lateral (in-plane) protein expansion of ~20 nm^2 (59), that makes the activation curve very steep, such that the equilibrium Po/Pc ratio changes 120 fold per every mN/m. MscL has also been shown to be very sensitive to the pressure profile in the surrounding bilayer as it can be activated by asymmetrically incorporated lysolipids (11) predicted to decrease local pressure in the hydrocarbon. It appears that Gd^{3+} does the opposite. We argue that the Gd^{3+}-induced lipid compaction can either redistribute pressure inside the bilayer to the hydrocarbon, or formation of solid domains can negate a large fraction of tension reaching the channel.

In a liquid bilayer uniformly compacted by Gd^{3+}, we expect primarily a redistribution of pressure to the hydrocarbon, with the total tension remaining the same. As shown in Fig. 2, porcine brain PS undergoes an 11% area compaction largely remaining in the liquid state. Extrapolation of the control curve to the left, from 57.3 $Å^2$ observed at 35 mN/m to 50.6 $Å^2$, predicts a pressure increase to ~45 mN/m, i.e., by 10 mN/m. Because this is the magnitude of the spontaneous compaction with 10 μm Gd^{3+} acting at the headgroups, the pressure in the hydrocarbon (not directly affected by Gd^{3+}) should increase by ~10 mN/m. For a bilayer, this should double to 20 mN/m and when divided by the thickness of the hydrocarbon (~3 nm), the extra pressure is estimated as 67 atm. This pressure, redistributed from the compacted headgroups to the hydrocarbon (4), would be pressing on the gate of the channel located in the core of the membrane. However, if the Gd^{3+}-compacted domain around the channel is small and well segregated from the surrounding lipids, then the line tension at the domain boundary would increase lateral pressure inside. With the domain radius of 3 nm and line tension (σ) of 5 pN, the lateral pressure inside the domain would be 1.5 mN/m higher, according to two-dimensional Laplace equation ($\sigma = \Delta\gamma/r$).

If the Gd^{3+}-affected domain becomes solid, then the physics changes. A protein completely surrounded by a shrinking solid PS domain would experience a constricting pressure as illustrated in Fig. S4. An exact analytical solution for the pressure p acting on a cylindrical protein of radius r inserted in the center of a discoid lipid domain undergoing condensation is given by the following equation:

$$p = \frac{E\alpha\left(1 - r^2/R^2\right)}{(1 + \sigma)\left[1 + r^2/R^2(1 - 2\sigma)\right]}, \qquad (1)$$

where r and R are the radii of the inclusion and the lipid domain, respectively, E and σ are the isothermal area compressibility coefficient and Poisson's ratio for the lipid domain in its condensed state, and $\alpha = \Delta 1/1$ is the relative linear contraction on ion binding (see derivation in the Supporting Material). Because the strain in the lipid will quickly decrease with the distance from the inclusion wall, p will weakly depend on R, if the lipid domain is large, but in the small domain where $r/R \sim 1$, p may critically depend on the number of lipid molecules in it. Assuming that the domain is sufficiently large ($r/R << 1$), and given typical numbers for lipids $E = 800$ mN/m measured for DMPC in the condensed gel state (60), $\sigma = 0.1$, and $\alpha = 0.1$ (area shrinkage by 19%), the pressure compressing the protein from all sides in x-y plane estimates as ~80 dyn/cm, which is one order of magnitude higher than tension activating MscL (10–12 dyn/cm). If the area compressibility modulus is lower (~200 mN/m) as for SOPC (53), we still obtain pressures in the order of 10 mM/m, which is sufficient to keep MscL closed at any attainable tension.

When the shrinking domain does not encircle the channel completely, the blocking effect may not be observed, and thus concentration of the ion-binding lipid species in the vicinity of a channel matters. The model used in this study does not specify the chemical nature of lipid-ligand interactions, and any type of binding that changes the equilibrium distance between molecules is expected to exert some effect on the channel gating.

All the scenarios of MscL blocking discussed above would be possible when PS was clustered around the protein. This requirement corroborates with the reports that the protein tends to coordinate negatively charged lipids in its annular layer (61,62). This poses the question of whether Gd^{3+} could induce phase separation and recruit more PS in a domain surrounding the protein. It would require a further study to determine whether Gd^{3+} creates PS clusters and whether MscL or other membrane proteins may nucleate formation of PS clusters around them and thus become sensitized to Gd^{3+}.

CONCLUSIONS

We have shown that blocking of liposome-reconstituted MscL by Gd^{3+} requires the presence of PS in the bilayer, and the data obtained from liposomes and monolayers indicated that PS molecules can form high-affinity binding sites for Gd^{3+} and likely other lanthanides. Gd^{3+} binging changes physical properties of the bilayer leaving the possibility that lanthanides can act locally on isolated PS domains altering functional properties of the resident transmembrane proteins. What needs to be clarified is whether PS is unique in this capacity to provide a ''receptive field'' for such ions, or other anionic lipids may do the same. Our unpublished data (Y. Ermakov and V. Shapovalov, unpublished) suggest that phosphatidylglycerol may act in a similar way. Also, the potency of other di- and trivalent ions as blockers should be studied in a similar context.

Monolayer experiments illustrate a strong Gd^{3+}-induced lateral condensation of phophatidylserines. The 11%

compaction of brain PS (Fig. 2) was not associated with isothermal phase transition, whereas DMPS films were spontaneously condensed to the limiting 40 $Å^2$ per lipid corresponding to the gel state (Fig. 3). In the previous studies of La^{3+} binding, it has been shown that both carboxyl and phosphate groups of phosphatidylserine participate in the ion coordination (38). Assuming that one PS molecule can potentially coordinate two different ions with its separate phosphate and carboxyl groups and each ion should be coordinated by at least three PS groups, this may explain the cross-linking potency of Gd^{3+} toward lamellar assemblies of PS in both membranes and monolayers.

The benchmark experiments (Fig. S1, Fig. S2, and Fig. S3) emphasized a drastic difference between DMPS and DMPC and showed that simple neutralization of PS headgroups makes the film more compressible, but does not cause compaction as strong as Gd^{3+}. Not delocalized electrostatics but rather tight ion coordination causes Gd^{3+}-induced film condensation and cross-linking. Metal binding, therefore, can be effectively converted by charged phospholipids into mechanical contraction and dipole polarization of the surface.

It has been known that water at the membrane interface contributes to the packing of lipids and magnitude of interfacial dipole potential (54). ITC experiments showed that Gd^{3+} binding to gel-like PS can be driven by entropy, most likely through liberation of water hydrating the headgroups and ions. At the same time, the Volta-potential measurements show that adsorption of Gd^{3+} produces only a modest effect (~18%) on dipole moments of individual headgroups, whereas the large overall dipole effect is mainly due to the density change. The good correspondence with the previous data obtained on natural brain PS (28) strongly suggests that the observed Gd^{3+}- induced dipole effects are headgroup-specific and are qualitatively similar in lipids with a different degree of acyl chain unsaturation. Compaction, which may be smaller in nonsaturated lipids, occurs without a cooperative phase transition observed in DMPS.

Saturation of the negative heat effect in ITC experiment occurred at Gd^{3+} concentrations near the isoelectric point for the surface, which was estimated previously as ~50 μM (28). This correspondence between thermochemical and electrostatic approaches supports the binding stoichiometry of 1 Gd^{3+} per the PS headgroups. The response of liquid DMPS to Gd^{3+} is especially sharp because the solidifying phase transition in this lipid is highly cooperative. The large negative heat effect seems to result from ion binding at the surface that condenses the hydrocarbon inside the bilayer. This prompts quantitative measurements of the mechanical and thermal behavior of individual nonsaturated PS species that exhibit less cooperative phase transitions at lower temperatures.

The observed compaction of PS by Gd^{3+} seems to be the most probable mechanism of its blocking effect on mechanosensitive channels. By pulling the headgroups together, Gd^{3+} is expected to generate extra pressure in the hydrocarbon core that would stabilize the narrow closed state of the channel. The coordination of multiple headgroup at a shorter distance by this ion is equivalent to imposing a strong negative spontaneous curvature to the lipids (63). The question is whether the increased lateral pressure is the only way Gd^{3+} affects the channels. As was suggested by one of the reviewers, Gd^{3+} may bias the open-closed equilibrium by changing the line tension at the protein-lipid boundary in one of the states (open or closed). This implies that PS headgroups present at the boundary should favorably interact with the open conformation, whereas Gd^{3+} may change the energy of the state by intercepting some ionic interactions or hydrogen bonds. This interesting perspective would require introduction of line tension into the equation for channel energy (59) and a systematic study of headgroup-dependency of MscL activation (12,62), which are beyond the scope of his study.

SUPPORTING MATERIAL

Methods and materials and four figures are available at http://www.biophysj.org/biophysj/supplemental/S0006-3495(09)06004-4.

We acknowledge a substantial contribution of Dr. Vladimir Shapovalov (Institute of Chemical Physics, Moscow) in experimental measurements on lipid monolayers presented in this study. The authors thank Drs. A. Anishkin and V. Yakovenko for discussions of mechanical properties of bilayers.

The study was supported in part by the Russian Foundation for Basic Research (07-03-00630 to Yu.E.) and the National Institutes of Health (2R01 NS03931405A to S.S.).

REFERENCES

1. Cantor, R. S. 1999. The influence of membrane lateral pressures on simple geometric models of protein conformational equilibria. *Chem. Phys. Lipids.* 101:45–56.
2. Botelho, A. V., T. Huber, …, M. F. Brown. 2006. Curvature and hydrophobic forces drive oligomerization and modulate activity of rhodopsin in membranes. *Biophys. J.* 91:4464–4477.
3. van den Brink-van der Laan, E., J. A. Killian, and B. de Kruijff. 2004. Nonbilayer lipids affect peripheral and integral membrane proteins via changes in the lateral pressure profile. *Biochim. Biophys. Acta.* 1666:275–288.
4. Cantor, R. S. 1998. The lateral pressure profile in membranes: a physical mechanism of general anesthesia. *Toxicol. Lett.* 100–101:451–458.
5. Carrillo-Tripp, M., and S. E. Feller. 2005. Evidence for a mechanism by which omega-3 polyunsaturated lipids may affect membrane protein function. *Biochemistry.* 44:10164–10169.
6. Gullingsrud, J., and K. Schulten. 2004. Lipid bilayer pressure profiles and mechanosensitive channel gating. *Biophys. J.* 86:3496–3509.
7. Ollila, O. H., H. J. Risselada, M. Louhivuori, E. Lindahl, I. Vattulainen, and S. J. Marrink. 2009. 3D pressure field in lipid membranes and membrane-protein complexes. *Phys. Rev. Lett.* 102:78–101.
8. Martinac, B., J. Adler, and C. Kung. 1990. Mechanosensitive ion channels of *E. coli* activated by amphipaths. *Nature.* 348:261–263.
9. Sukharev, S. I., W. J. Sigurdson, …, F. Sachs. 1999. Energetic and spatial parameters for gating of the bacterial large conductance mechanosensitive channel, MscL. *J. Gen. Physiol.* 113:525–540.

10. Sukharev, S. 2002. Purification of the small mechanosensitive channel of *Escherichia coli* (MscS): the subunit structure, conduction, and gating characteristics in liposomes. *Biophys. J.* 83:290–298.

11. Perozo, E., A. Kloda, …, B. Martinac. 2002. Physical principles underlying the transduction of bilayer deformation forces during mechanosensitive channel gating. *Nat. Struct. Biol.* 9:696–703.

12. Moe, P., and P. Blount. 2005. Assessment of potential stimuli for mechano-dependent gating of MscL: effects of pressure, tension, and lipid headgroups. *Biochemistry.* 44:12239–12244.

13. Li, X. M., Y. F. Zhang, …, F. Hwang. 1994. Effect of lanthanide ions on the phase behavior of dipalmitoylphosphatidylcholine multilamellar liposomes. *J. Inorg. Biochem.* 53:139–149.

14. Orlowski, S., F. Henao, and P. Champeil. 1992. Binding of gadolinium ions to sarcoplasmic reticulum membranes. *Ann. N. Y. Acad. Sci.* 671:421–423.

15. Bentz, J., D. Alford, …, N. Düzgüneş. 1988. La^{3+}-induced fusion of phosphatidylserine liposomes. Close approach, intermembrane intermediates, and the electrostatic surface potential. *Biophys. J.* 53: 593–607.

16. Cheng, Y., M. Liu, …, K. Wang. 1999. Gadolinium induces domain and pore formation of human erythrocyte membrane: an atomic force microscopic study. *Biochim. Biophys. Acta.* 1421:249–260.

17. Hammoudah, M. M., S. Nir, …, R. J. Kurland. 1981. Interactions of La^{2+} with phosphatidylserine vesicles: binding, phase transition, leakage, ^{31}P-NMR and fusion. *Biochim. Biophys. Acta.* 645:102–114.

18. Tanaka, T., Y. Tamba, …, M. Yamazaki. 2002. La(3+) and Gd(3+) induce shape change of giant unilamellar vesicles of phosphatidylcholine. *Biochim. Biophys. Acta.* 1564:173–182.

19. Alexy, T., N. Nemeth, …, H. J. Meiselman. 2007. Effect of lanthanum on red blood cell deformability. *Biorheology.* 44:361–373.

20. Millet, B., and B. G. Pickard. 1988. Gadolinium ion is an inhibitor suitable for testing the putative role of stretch-activated ion channels in geotropism and thigmotropism. *Biophys. J.* 53:A155.

21. Ding, J. P., and B. G. Pickard. 1993. Mechanosensory calcium-selective cation channels in epidermal cells. *Plant J.* 3:83–110.

22. Yang, X. C., and F. Sachs. 1989. Block of stretch-activated ion channels in *Xenopus* oocytes by gadolinium and calcium ions. *Science.* 243:1068–1071.

23. Ruknudin, A., F. Sachs, and J. O. Bustamante. 1993. Stretch-activated ion channels in tissue-cultured chick heart. *Am. J. Physiol.* 264: H960–H972.

24. Hamill, O. P., and D. W. McBride, Jr. 1996. The pharmacology of mechanogated membrane ion channels. *Pharmacol. Rev.* 48:231–252.

25. Oliet, S. H., and C. W. Bourque. 1996. Gadolinium uncouples mechanical detection and osmoreceptor potential in supraoptic neurons. *Neuron.* 16:175–181.

26. Terrian, D. M., D. S. Damron, …, R. L. Gannon. 1989. Effects of calcium antagonists on the evoked release of dynorphin A(1-8) and availability of intraterminal calcium in rat hippocampal mossy fiber synaptosomes. *Neurosci. Lett.* 106:322–327.

27. Shin, K. S., J. Y. Park, …, M. S. Kang. 1996. Involvement of K(Ca) channels and stretch-activated channels in calcium influx, triggering membrane fusion of chick embryonic myoblasts. *Dev. Biol.* 175: 14–23.

28. Ermakov, Y. A., A. Z. Averbakh, A. I. Yusipovich, and S. Sukharev. 2001. Dipole potentials indicate restructuring of the membrane interface induced by gadolinium and beryllium ions. *Biophys. J.* 80:1851–1862.

29. Vance, J. E. 2008. Phosphatidylserine and phosphatidylethanolamine in mammalian cells: two metabolically related aminophospholipids. *J. Lipid Res.* 49:1377–1387.

30. Johnson, J. E., J. Giorgione, and A. C. Newton. 2000. The C1 and C2 domains of protein kinase C are independent membrane targeting modules, with specificity for phosphatidylserine conferred by the C1 domain. *Biochemistry.* 39:11360–11369.

31. Wu, Y., N. Tibrewal, and R. B. Birge. 2006. Phosphatidylserine recognition by phagocytes: a view to a kill. *Trends Cell Biol.* 16:189–197.

32. Morrissey, J. H., V. Pureza, …, E. Tajkhorshid. 2008. Blood clotting reactions on nanoscale phospholipid bilayers. *Thromb. Res.* 122 (*Suppl 1*):S23–S26.

33. Slater, S. J., C. Ho, …, C. D. Stubbs. 1993. Contribution of hydrogen bonding to lipid-lipid interactions in membranes and the role of lipid order: effects of cholesterol, increased phospholipid unsaturation, and ethanol. *Biochemistry.* 32:3714–3721.

34. Bakht, O., P. Pathak, and E. London. 2007. Effect of the structure of lipids favoring disordered domain formation on the stability of cholesterol-containing ordered domains (lipid rafts): identification of multiple raft-stabilization mechanisms. *Biophys. J.* 93:4307–4318.

35. Cevc, G., A. Watts, and D. Marsh. 1981. Titration of the phase transition of phosphatidylserine bilayer membranes. Effects of pH, surface electrostatics, ion binding, and head-group hydration. *Biochemistry.* 20:4955–4965.

36. Mattai, J., H. Hauser, …, G. G. Shipley. 1989. Interactions of metal ions with phosphatidylserine bilayer membranes: effect of hydrocarbon chain unsaturation. *Biochemistry.* 28:2322–2330.

37. Verstraeten, S. V., L. V. Nogueira, …, P. I. Oteiza. 1997. Effect of trivalent metal ions on phase separation and membrane lipid packing: role in lipid peroxidation. *Arch. Biochem. Biophys.* 338:121–127.

38. Petersheim, M., and J. Sun. 1989. On the coordination of La^{3+} by phosphatidylserine. *Biophys. J.* 55:631–636.

39. Ermakov, Y. A., and A. I. Yusipovich. 2002. Boundary potential and tension of planar BLM in the presence of gadolinium measurements in the condition of instant perfusion of the cell. *Biol. Membrany.* 19:499–506.

40. Träuble, H., and H. Eibl. 1974. Electrostatic effects on lipid phase transitions: membrane structure and ionic environment. *Proc. Natl. Acad. Sci. USA.* 71:214–219.

41. Casal, H. L., H. H. Mantsch, …, H. Hauser. 1987. Infrared and ^{31}P-NMR studies of the effect of Li^{+} and Ca^{2+} on phosphatidylserines. *Biochim. Biophys. Acta.* 919:275–286.

42. Demel, R. A., F. Paltauf, and H. Hauser. 1987. Monolayer characteristics and thermal behavior of natural and synthetic phosphatidylserines. *Biochemistry.* 26:8659–8665.

43. Dahim, M., N. K. Mizuno, …, H. L. Brockman. 2002. Physical and photophysical characterization of a BODIPY phosphatidylcholine as a membrane probe. *Biophys. J.* 83:1511–1524.

44. Smaby, J. M., M. M. Momsen, …, R. E. Brown. 1997. Phosphatidylcholine acyl unsaturation modulates the decrease in interfacial elasticity induced by cholesterol. *Biophys. J.* 73:1492–1505.

45. Cevc, G., and D. Marsh. 1987. Phospholipid Bilayers. *In* Physical Principles and Models.. J. Wiley & Sons, New York, NY.

46. Tocanne, J. F., and J. Teissié. 1990. Ionization of phospholipids and phospholipid-supported interfacial lateral diffusion of protons in membrane model systems. *Biochim. Biophys. Acta.* 1031:111–142.

47. Ermakov, Yu. A., A. Z. Averbakh, and S. I. Sukharev. 1997. Lipid and cell membranes in the presence of gadolinium and other ions with high affinity to lipids. 1. Dipole and diffuse components of the boundary potential. *Membr. Cell Biol.* 11:539–554.

48. Ali, S., J. M. Smaby, …, R. E. Brown. 1998. Acyl chain-length asymmetry alters the interfacial elastic interactions of phosphatidylcholines. *Biophys. J.* 74:338–348.

49. Leberle, K., I. Kempf, and G. Zundel. 1989. An intramolecular hydrogen bond with large proton polarizability within the head group of phosphatidylserine. An infrared investigation. *Biophys. J.* 55:637–648.

50. McLaughlin, S. 1989. The electrostatic properties of membranes. *Annu. Rev. Biophys. Biophys. Chem.* 18:113–136.

51. Smaby, J. M., and H. L. Brockman. 1990. Surface dipole moments of lipids at the argon-water interface. Similarities among glycerol-ester-based lipids. *Biophys. J.* 58:195–204.

52. Brockman, H. 1994. Dipole potential of lipid membranes. *Chem. Phys. Lipids.* 73:57–79.

53. Marsh, D. 1990. Handbook of Lipid Bilayers. CRC Press, Boca Raton, FL.

54. Gawrisch, K., D. Ruston, …, N. Fuller. 1992. Membrane dipole potentials, hydration forces, and the ordering of water at membrane surfaces. *Biophys. J.* 61:1213–1223.

55. Zhou, F., and K. Schulten. 1995. Molecular-dynamics study of a membrane water interface. *J. Phys. Chem.* 99:2194–2207.

56. Ramsay, G., R. Prabhu, and E. Freire. 1986. Direct measurement of the energetics of association between myelin basic protein and phosphatidylserine vesicles. *Biochemistry.* 25:2265–2270.

57. Torrecillas, A., J. Laynez, …, J. C. Gómez-Fernández. 2004. Calorimetric study of the interaction of the C2 domains of classical protein kinase C isoenzymes with Ca^{2+} and phospholipids. *Biochemistry.* 43:11727–11739.

58. López-García, F., J. Villalaín, and J. C. Gómez-Fernández. 1994. Diacylglycerol, phosphatidylserine and Ca^{2+}: a phase behavior study. *Biochim. Biophys. Acta.* 1190:264–272.

59. Chiang, C. S., A. Anishkin, and S. Sukharev. 2004. Gating of the large mechanosensitive channel in situ: estimation of the spatial scale of the transition from channel population responses. *Biophys. J.* 86: 2846–2861.

60. Evans, E., and D. Needham. 1986. Giant vesicle bilayers composed of mixtures of lipids, cholesterol and polypeptides. Thermomechanical and (mutual) adherence properties. *Faraday Discuss. Chem. Soc.* 81: 267–280.

61. Powl, A. M., J. M. East, and A. G. Lee. 2005. Heterogeneity in the binding of lipid molecules to the surface of a membrane protein: hot spots for anionic lipids on the mechanosensitive channel of large conductance MscL and effects on conformation. *Biochemistry.* 44:5873–5883.

62. Powl, A. M., J. M. East, and A. G. Lee. 2008. Anionic phospholipids affect the rate and extent of flux through the mechanosensitive channel of large conductance MscL. *Biochemistry.* 47:4317–4328.

63. Marsh, D. 2007. Lateral pressure profile, spontaneous curvature frustration, and the incorporation and conformation of proteins in membranes. *Biophys. J.* 93:3884–3899.